Review of OCA activities on nulling testbench PERSEE

François Hénault[a], Paul Girard[b], Aurélie Marcotto[a], Nicolas Mauclert[a], Christophe Bailet[a], Jean-Michel Clausse[a], Denis Mourard[a], Yves Rabbia[a], Alain Roussel[a], Marc Barillot[c] and Jean-Michel Le Duigou[d]

[a] UMR 6525 CNRS H. Fizeau, UNS, OCA, Avenue Nicolas Copernic, 06130 Grasse – France
[b] Observatoire de la Côte d'Azur, Boulevard de l'Observatoire, 06304 Nice – France
[c] Thales Alenia Space, 100 Boulevard du Midi, 06322 Cannes-la-Bocca – France
[d] Centre National d'Etudes Spatiales, 18 Avenue Edouard Belin, 31401 Toulouse – France

ABSTRACT

We present a review of our activities on PERSEE (Pégase Experiment for Research and Stabilization of Extreme Extinction) at Observatoire de la Côte d'Azur (OCA). PERSEE is a laboratory testbench aiming at achieving a stabilized nulling ratio better than 10^{-4} in the astronomical bands K and M, in presence of flight-representative spacecraft perturbations. The bench has been jointly developed by a Consortium of six French institutes and companies, among which OCA was responsible for the star simulator and of the opto-mechanical studies, procurement and manufacturing of the optical train. In this communication are presented the alignment and image quality requirements and the opto-mechanical design of the illumination module and main optical train, including a periscope Achromatic Phase Shifter (APS), tip-tilt mirrors used to introduce and then compensate for dynamic perturbations, delay lines, beam compressors and fiber injection optics. Preliminary test results of the star simulator are also provided.

Keywords: Nulling interferometry, Nulling testbench, Achromatic phase shifter, Opto-mechanical design

1 INTRODUCTION

Nulling interferometry is nowadays a widely known and studied technique, aiming at discovering Earth-like planets orbiting around nearby stars in their habitable zone, and characterizing their atmospheres in hope of recognizing signs of life. During the last decade, the European Space Agency (ESA) and National Aeronautics and Space Administration (NASA) extensively developed two major projects of spaceborne nulling interferometers respectively named Darwin [1] and TPF-I (Terrestrial Planet Finder Interferometer [2]). But these systems are so demanding in terms of technical and operational requirements that a gradual approach comprising several intermediate steps such as laboratory demonstrators and space validation missions seems absolutely mandatory. This is the reason why less ambitious instruments such as the Fourier Kelvin Stellar Interferometer (FKSI) [3] in the USA or Pégase [4] in France have been considered as precursors for TPF-I and Darwin, in order to validate the most of critical technologies such as Optical Path Difference (OPD) control at nanometric level or spacecrafts free-flying in formation within an accuracy of a few millimeters. In addition, these instruments will also enable to characterize the exo-zodiacal clouds of the target extra-solar systems as well as detecting and spectrally analyzing the atmosphere of their Jupiter-like planets.

In this perspective, the French Centre National d'Etudes Spatiales (CNES) has undertaken the development of a laboratory nulling testbench named PERSEE, an acronym standing for "Pégase Experiment for Research and Stabilization of Extreme Extinction" [5]. In charge of the project management and system analyses, CNES is actually leading a Consortium of five institutes and companies, whose main responsibilities are listed below:

- The Observatoire de la Côte d'Azur (OCA) is in charge of the illumination module and star simulator, and more generally of the procurement and testing of most of the opto-mechanical components equipping the bench, together constituting the main optical train, at the exception of the recombining optics.

- OCA is helped in this task by the industrial company Thales Alenia Space who defined the mechanical architecture of the whole testbench and realized its CAD model.
- The Institut d'Astrophysique Spatiale (IAS) is in charge of the procurement, alignment and testing of the axially recombining optics, which consists in a Modified Mach-Zehnder (MMZ) interferometer.
- The Office National d'Etudes et Recherches Aérospatiales (ONERA) has the responsibility of the fringe and tip-tilt sensors that are used to monitor the opto-mechanical disturbances, and of the control software of the whole testbench.
- Lastly, the LESIA laboratory of Observatoire de Paris is responsible for the IR camera, and of the final Assembly, Integration and Test (AIT) sequence that is being carried out in one of his clean rooms in Meudon.

The purpose of this paper is to present a review of the main OCA activities that have been performed for four years on the nulling testbench PERSEE, including in section 2 a general description of the bench, the definition of the opto-mechanical alignment and image quality requirements, and the design of a chromatism compensator being convertible into an Achromatic Phase Shifter (APS). Section 3 presents the design of the star simulator and the first obtained test results, while section 4 focuses on the opto-mechanical conception of the main optical train. It must be highlighted that another paper is presented in this conference, dealing in great detail with the first experimental results obtained from the PERSEE nulling testbench [6].

2 GENERAL DESCRIPTION

2.1 PERSEE optical layout

The major technical requirements of PERSEE have been extensively detailed in ref. [5] and could be roughly summarized as follows: to demonstrate a nulling ratio better than 10^{-4} in the full astronomical bands K and M, stabilized within 10^{-5} on durations of typically several hours, in presence of OPD and tip-tilt disturbances being representative of spacecrafts flying in formation. Below are listed the main components of the testbench, whose optical layout is schematically illustrated on Figure 1. The PERSEE experiment is actually deployed on three different optical tables, connected together by means of optical fibers:

1) An illumination module includes all the necessary light sources to optically feed the interferometer in the required spectral bands. This light sources module is further described in section 3.
2) The main interferometer bench gathers all the opto-mechanical components required to simulate the three Pégase spacecrafts from collection of the star photons by two siderostats up to recombination and final injection of the beams into single-mode fibers (SMFs) spatially filtering the instrumental wavefront errors (WFEs). The detailed description of its major components is provided below.
3) Lastly, a separate optical table, namely the detection module, hosts an infrared CCD camera equipped with a low-dispersion prism splitting the bright and nulled output beams of the interferometer over the desired spectral range.

The design of the main interferometer is essentially based on one of the classical symmetric configurations originally discussed by Serabyn, making use of a Mach-Zehnder coaxial combiner [7], a technique that has been shown to be superior in terms of achievable throughput for the observed planets [8]. In addition, the natural arrangement of the two collecting telescopes of Pégase already provides the first stage of a periscopic achromatic phase shifter, hence this APS concept has been preferred with respect to other existing designs (it must be noted, however, that a dioptric APS made of four dispersive plates was selected as a backup solution that can be easily implemented on the testbench, see § 2.3). Following the path and sense of starlight photons, the successively encountered optical elements are the following:

- The central star is simulated by means of an optical fiber that is single-mode in the K and M bands, and put at the focus of a parabolic mirror M0. A diaphragm pierced with two holes defines two separate beams at the exit of the collimating optics.

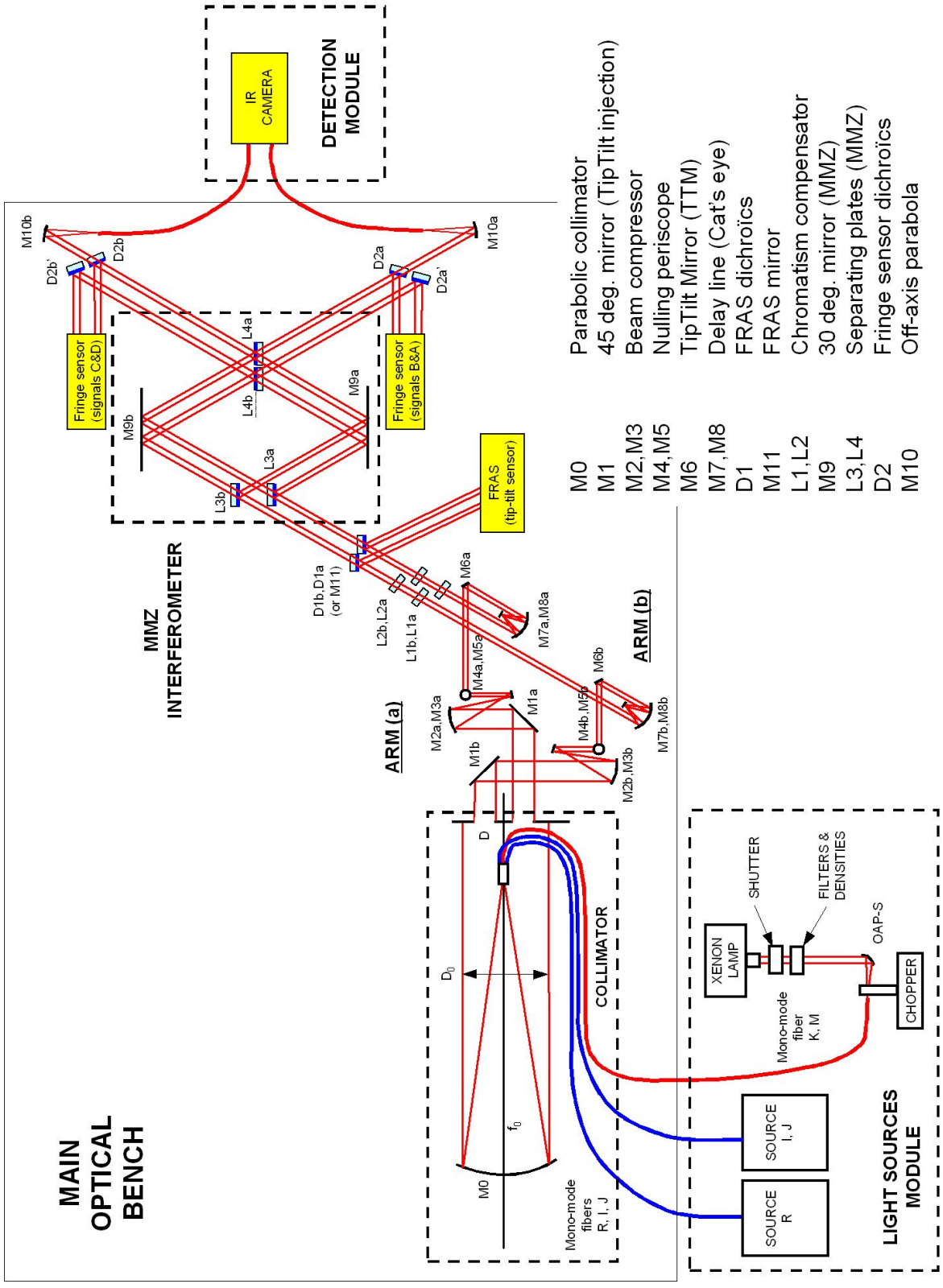

Figure 1: Optical layout of PERSEE interferometer.

- A couple of 45-degs. tilted, flat mirrors M1a and M1b materializes the two Pégase siderostats, and are used to inject into the interferometer OPD and tip-tilt perturbations that are representative of spacecrafts alignment drifts and micro-vibrations generated by their reaction wheels. These perturbations will be compensated for downstream by optical delay lines (ODLs) and M6 tip-tilt mirrors, respectively.
- Two afocal beam compressors, each being constituted of a couple of off-axis parabolic mirrors (M2a, M3a) and (M2b M3b), are representing the compressing optics that should be integrated into the central combining spacecraft of Pégase.
- Two couples of 45-degs. tilted, flat mirrors (M4a, M5a) and (M4b M5b) are standing for the second stage of the periscopic APS, introducing an achromatic phase-shift equal to π between both interferometer arms (a) and (b).
- A couple of 30-degs. tilted, flat mirrors M6a and M6b are mounted on piezzo-electrically driven, tip-tilt stages, in charge of compensating for alignment errors introduced upstream by the M1s and measured downstream by the Field Relative Angle Sensor (FRAS), which is the actual tip-tilt sensor of the testbench. It has to be noticed that these mirrors are also conjugated with the physical aperture stop of the whole optical system that is located behind the MMZ.
- Next, two ODLs are employed to compensate for OPD disturbances injected by the M1s and measured by a couple of fringe sensors (FS) located near two of the MMZ output ports. Each ODL is of the cat's eye type, being composed of parabolic concave mirrors M7a and M7b, and of spherical convex mirrors M8a and M8b.
- On each interferometer arm, a fraction of the incident flux is then reflected toward the tip-tilt sensor by a staircase mirror M11.
- Two couples of compensating plates (L1a, L2a) and (L1b, L2b) are located just before the axial recombiner and are utilized for fine chromatism compensation, or for achromatically phase-shifting the optical beams (§ 2.3).
- The axial combiner itself is a MMZ interferometer that has been fully described in ref. [9].
- At the MMZ outputs, four small dichroïcs plates (D2a, D2a', D2b, D2b') are reflecting the lower region of the electro-magnetic spectrum in the direction of the FSs, while transmitting both the bright and nulled infrared beams to the M10 injection mirrors.
- Finally, a couple of off-axis parabolic mirrors M10a and M10b inject the output beams into two single-mode optical fibers, conveying the exit photons to the IR camera located on the detection module and filtering the WFEs of the testbench.

In the following section are briefly summarized the major technical requirements of most of the previous optical components.

2.2 Alignment and image quality requirements

Defining and quantifying the alignment and image quality requirements of all the opto-mechanical components of PERSEE was a long task that has been shared between all Consortium partners, and is summarized in ref. [10]. Table 1 gives a rapid overview of the resulting alignment tolerances applicable to the main units in the optical train, for all degrees of freedom in translation and rotation. All the figures include manufacturing, positioning and alignment accuracy as well as their short and long-term stability. Dark cells indicate those cases when the use of alignment stages could not be avoided, although we seek to restrict their number as much as possible in order to simplify the adjustment procedure and to limit the risks of accidental misalignment. In most cases, these requirements could be deduced from rather simple and quickly calculable criteria such as:

- Optical axis alignment for the collimating optics M0, the M7 and M8 mirrors of the ODL, the staircase mirror M11 and dichroïcs D2,
- Flux balance between both interferometer arms for M0 tilts,
- Required finesse of chromatism compensation for L1 and L2.

Another important criteria was the radiometric efficiency of the whole system, which is essentially driven by the coupling ratio of the beams into the output SMFs (it self being linked to the Strehl ratio of the optics), thus allowing to determine acceptable misalignments for ODL, M10 and SMF fiber heads. Image quality requirements summarized on Table 2 were also derived from the same criterion, leading to reasonable polishing accuracies thanks to the WFE filtering ability of the SMFs and the selected, near IR spectral bands. Only the definition of tilt requirements of most mirrors, which are primarily originating from differential polarization constraints, needed the development of a full non-sequential ZEMAX model of the interferometer carried out by CNES [10].

POSITIONING ACCURACY	Lateral translations (decenters)	Axial translation (defocus)	Tilts	Roll angle	Driving requirements
Input SMF	**1 µm**	**10 µm**	**30 arcsec**	5 degs.	Optical axis alignment and flux balance
M0	0.5 mm	0.5 mm	**3 arcsec**	5 degs.	Optical axis alignment and flux balance
M1a, M1b	0.5 mm	0.5 mm	**3 arcsec**	5 degs.	Differential polarization
M2a, M2b	**10 µm**	0.5 mm	**3 arcsec**	1 deg.	Differential polarization
M3a, M3b	0.5 mm	**10 µm**	**3 arcsec**	1 deg.	Differential polarization
M4a, M4b	0,5 mm	0,5 mm	**3 arcsec**	5 degs.	Differential polarization
M5a, M5b	0,5 mm	0,5 mm	**3 arcsec**	5 degs.	Differential polarization
M6a, M6b	**10 µm**	0,5 mm	**3 arcsec**	5 degs.	Differential polarization
Delay lines	0,5 mm	0,5 mm	1 deg.	5 degs.	
M7a, M7b	0.5 mm	0.5 mm	**3 arcsec**	5 degs.	Optical axis alignment and image quality
M8a, M8b	**10 µm**	**10 µm**	1 deg.	5 degs.	Optical axis alignment and image quality
L1a, L1b	**1 µm**	0,5 mm	30 arcmin	5 degs.	Accuracy of chromatism compensation
L2a, L2b	**1 µm**	0,5 mm	30 arcmin	5 degs.	Accuracy of chromatism compensation
M11	0,5 mm	0,5 mm	**3 arcsec**	5 degs.	Optical axis alignment
D2a, D2b	0,5 mm	0,5 mm	30 arcmin	5 degs.	Optical axis alignment
M10a, M10b	0,5 mm	0,5 mm	**10 arcsec**	1 deg.	Coupling ratio into SMF
Output SMFs	**0.3 µm**	**0.3 µm**	1 deg.	5 degs.	Coupling ratio into SMF

Alignment stages required

Table 1: Summary of alignment requirements.

Component	Type	Material/Coating	WFE (wavelengths @1.65 µm)	Manufacturing difficulty
M0	Parabolic mirror	Zerodur, unprotected gold coated	0.0153	Moderate
M1a, M1b	Flat mirror	Zerodur, unprotected gold coated	0.0153	Easy
M2a, M2b	Off-axis parabolic mirror	Zerodur, unprotected gold coated	0.0639	Moderate
M3a, M3b	Off-axis parabolic mirror	Zerodur, unprotected gold coated	0.0639	Moderate
M4a, M4b	Flat mirror	Zerodur, unprotected gold coated	0.0153	Easy
M5a, M5b	Flat mirror	Zerodur, unprotected gold coated	0.0153	Easy
M6a, M6b	Flat mirror	Zerodur, unprotected gold coated	0.0153	Easy
M7a, M7b	Parabolic mirror	Zerodur, unprotected gold coated	0.0320	Moderate
M8a, M8b	Parabolic mirror	Zerodur, unprotected gold coated	0.0153	Easy
L1a, L1b	Wedged plate	CAF2, uncoated	0.0014	Easy
L2a, L2b	Wedged plate	CAF2, uncoated	0.0014	Easy
M11	Flat mirror	Zerodur, unprotected gold coated	0.0153	Moderate
D2a, D2b	Dichroics	Fused silica, SR and AR coated	0.0028	Moderate
M10a, M10b	Off-axis parabolic mirror	Zerodur, unprotected gold coated	0.0639	Difficult
		Total WFE RMS	0.1222	**Requirement**
		Strehl ratio	0.479	> 0.40

Table 2: Summary of image quality requirements.

2.3 Chromatism Compensator (CC) and dioptric APS

As mentioned in section 2.1, the basic design selected for the PERSEE APS involves a periscopic arrangement of flat mirrors producing a pupil flip and a Field of View (FoV) inversion between both interferometer arms [7]. Although this design is particularly well-suited to the case of a two-telescopes, Bracewell interferometer such as Pégase, it suffers from

two identified drawbacks: first, the pupil flip induces a loss of spatial coherence, in turn reducing the effective FoV of the interferometer to a few off-axis bright fringes [11-12]. Secondly, these systems are reputed to be highly sensitive to optical misalignments and instabilities. For the both reasons and also due to the fact that a chromatism compensator is nevertheless needed for PERSEE in order to compensate for possible MMZ manufacturing errors, we decided to study the implementation of a glass plates CC that could be turned into a dioptric APS at a later stage. The principle of the dioptric APS that was originally proposed by Morgan *et al* [13] consists in equalizing the OPDs over a large spectral band by means of plane and parallel dispersive plates of different thicknesses and materials, using a technique related to the classical achromatisation of optical doublets. Later, the original design was improved by Veber *et al* [14] with the introduction of wedged glass plates (as shown on the left panel of Figure 2) in order to facilitate opto-mechanical alignments.

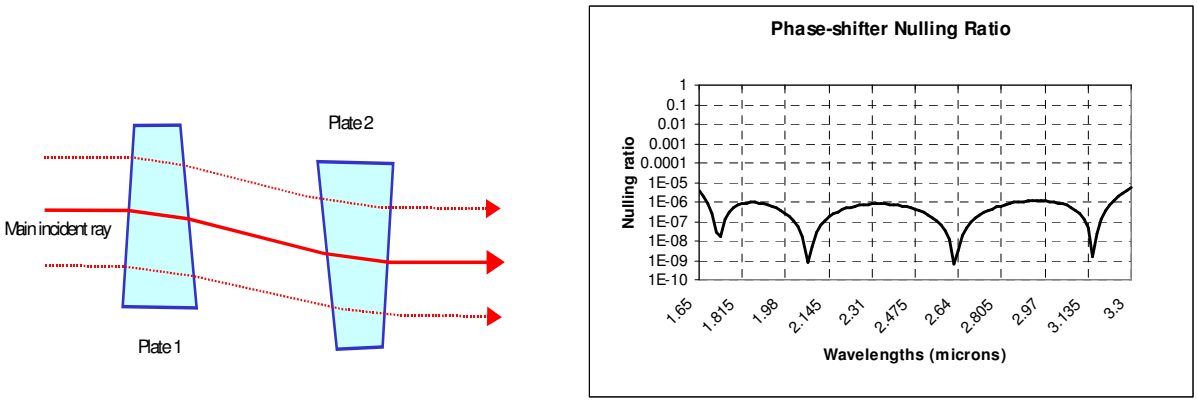

Figure 2: Schematic principle of CC/dioptric APS installed on both interferometer arms (left panel) and achievable nulling ratio with dioptric APS (right panel).

In our case, the material required for the CC must obviously be CaF2, since the latter had been selected for the separating and compensating plates equipping the MMZ [9]. The CC is thus constituted of four identical CaF2 wedged plates of type L1a indicated in Table 3 and arranged along each interferometer arm as depicted on the left panel of Figure 2. Owing to the retained parameters the CC is in principle able to cancel the residual chromatism of the MMZ plates with a $\pi/500$ accuracy over a $\pm 15\pi$ range, which corresponds to an equivalent optical plates or coatings thickness difference of 5 µm. The CC can easily be turned into a dioptric APS by replacing three L1a plates with the L2a, L1b and L2b plates specified in Table 3, two of them being made of fused silica material. The achievable nulling ratio on the K and M bands is then illustrated by the right panel of Figure 2 and is far within the PERSEE requirements.

In addition to nulling requirements, the design of a dioptric APS is also influenced by a few other factors such as:

- Parasitic reflections between both faces of the glass plates, herein corresponding to a coupled energy into the SMF lower than 10^{-6}.
- Angular deviations induced by the wedged plates, here limited to 1 arcsec on the full spectral band.
- Differential chromatism induced by the wedged plates, which was shown to be negligible.

	L1a	L2a	L1b	L2b
Material	CaF2	Fused Silica	CaF2	Fused Silica
Thickness	6 mm	6 mm	5.742 mm	6.056 mm
Prismatic angle	10 arcmin	-3.11 arcmin	10 arcmin	-3.11 arcmin
Alignment range	± 10 mm	No alignment	± 10 mm	No alignment

Table 3: Main parameters of APS glass plates. The dioptric APS can be turned into a chromatism compensator by replacing plates L2a, L1b and L2b with three identical L1a plates.

3 STAR SIMULATOR MODULE

Figure 3 presents a schematic view of the star simulator module (composed of the light sources module installed on a separated optical bench and the collimator described in § 2.1) and of its test hardware. The light sources module basically incorporates the following elements:

- The principal light source is a high-radiance, 75 W Xenon lamp from Lot-Oriel. This type of lamps was selected because their emitted spectra approximately match those of visible stars up to the near infrared domain.
- A set of spectral filters and densities allows one to adjust the flux levels and desired spectral bandwidths. The module also includes the general shutter of the whole PERSEE experiment that is remotely controlled.
- The light is then injected into a fluoride glass SMF specifically manufactured by Le Verre Fluoré (LVF, France), whose cut-off wavelength is 1.65 µm. The use of a mono-mode optical fiber in the star simulator module enables one to cancel the stellar leakage that would otherwise be generated by the finite size of the fiber core at the focus of the M0 parabola.
- Two auxiliary laser diodes (an Exalos at 1320 nm for the J band and a Thorlabs at 830 nm for the I band) are used for tip-tilt sensing and fringe tracking, respectively performed by the FRAS and FSs on the main optical bench. These metrology beams are filtered by two fused silica SMFs joining the LVF fiber by means of a customized connector located at the M0 focus. A red laser diode is also available for visual alignment purpose.
- The test hardware consists in a mono-pixel detector IGA-020-PSD from EOS system, mounted on two orthogonal translation stages located at the exit of the collimator, and a Stanford Research lock-in amplifier. All the electronic control-command and data recording exchanges are monitored by a Labview program.

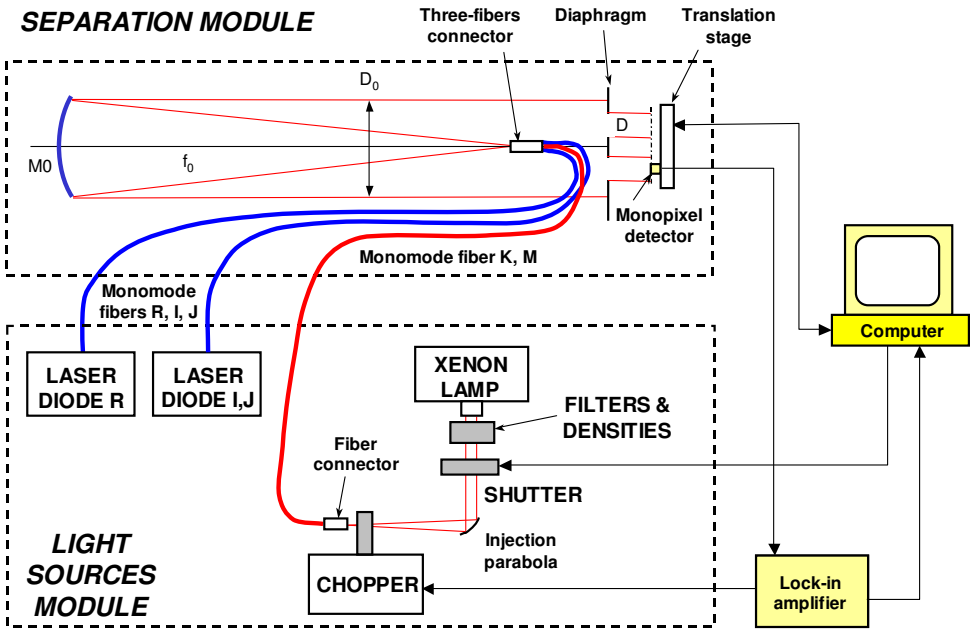

Figure 3: Design and test setup of star simulator module.

All mechanical parts of the star simulator have been entirely designed and manufactured by OCA. Figure 4 shows some pictures of the light source module and collimator tested on the optical laboratory. An example of irradiance map measured at the output of the star simulator module is reproduced on the bottom right panel of Figure 4. Despite of its

noisy aspect, it has been checked that the exit beam is still single-mode, and that flux differences between both interferometer arms can be lowered down to 1 %, which is compliant with system level requirements [10]. Next section will now provide a more detailed description of the opto-mechanical design and conception of the main optical train.

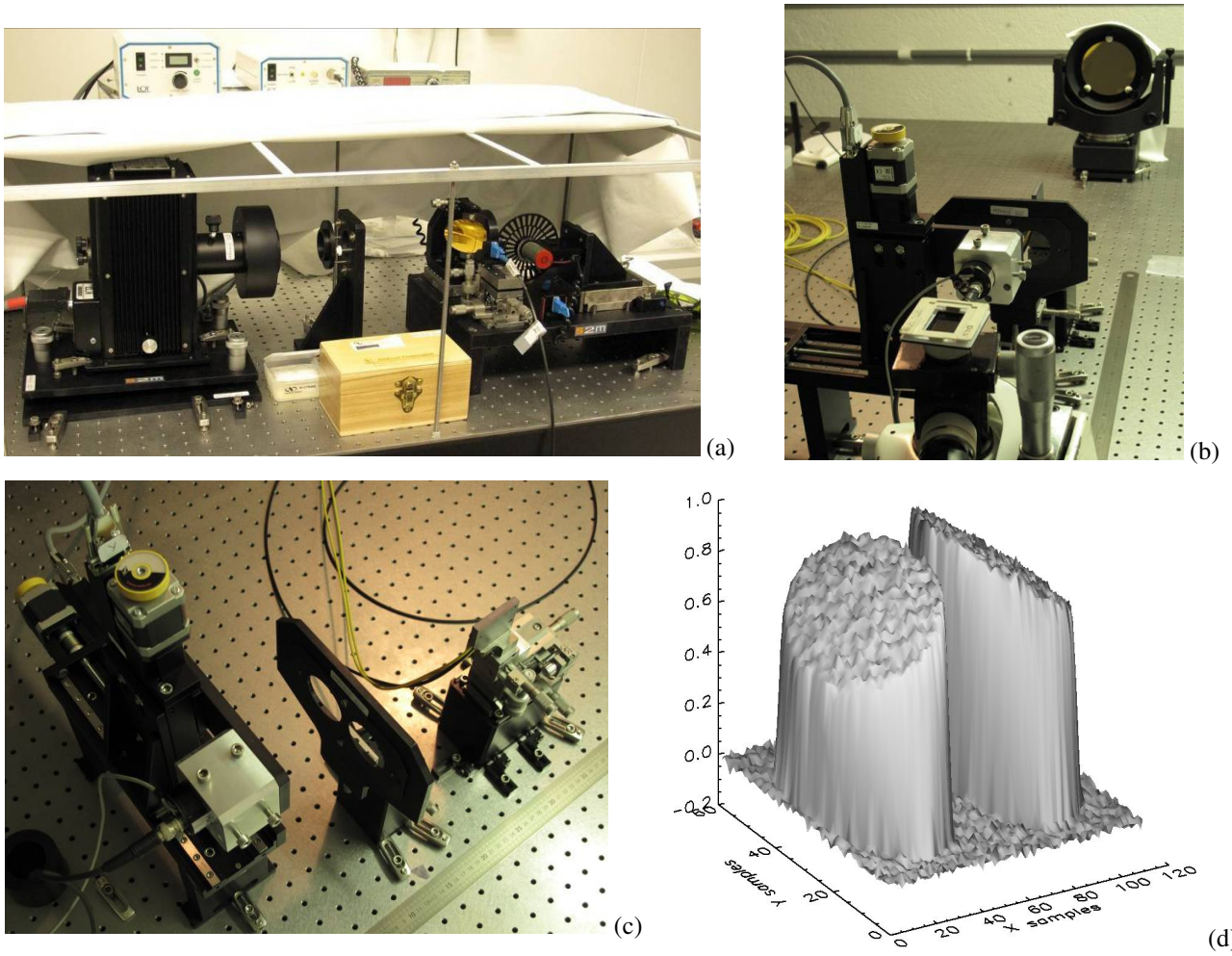

Figure 4: Integration of star simulator module. a) Light source module. b) Separation module tested on the optical bench. c) Test hardware. d) Measured irradiance map at the output of the collimator.

4 MAIN OPTICAL TRAIN

The mechanical design of the main optical train of PERSEE based on the optical study presented in section 2 is illustrated by the CAD view of Figure 5, and has been studied by Thales Alenia Space under OCA responsibility. The manufacturing of all PERSEE elements has been mainly achieved through our S2M (Service Mécanique Mutualisé, standing for shared mechanical workshop) up to 90%. In view of the large number of modules to be delivered, manufacturing has been planned according to the practical needs of the Consortium. Figure 7 and Figure 6 show some pictures of the realized hardware, whose approved elements were all tested individually on the site of Grasse in order to ensure their functioning and conformity to the alignment requirements of Table 1. This sequence included many measurements and tests performed on the optical laboratory such as illustrated on the bottom right panel of Figure 6.

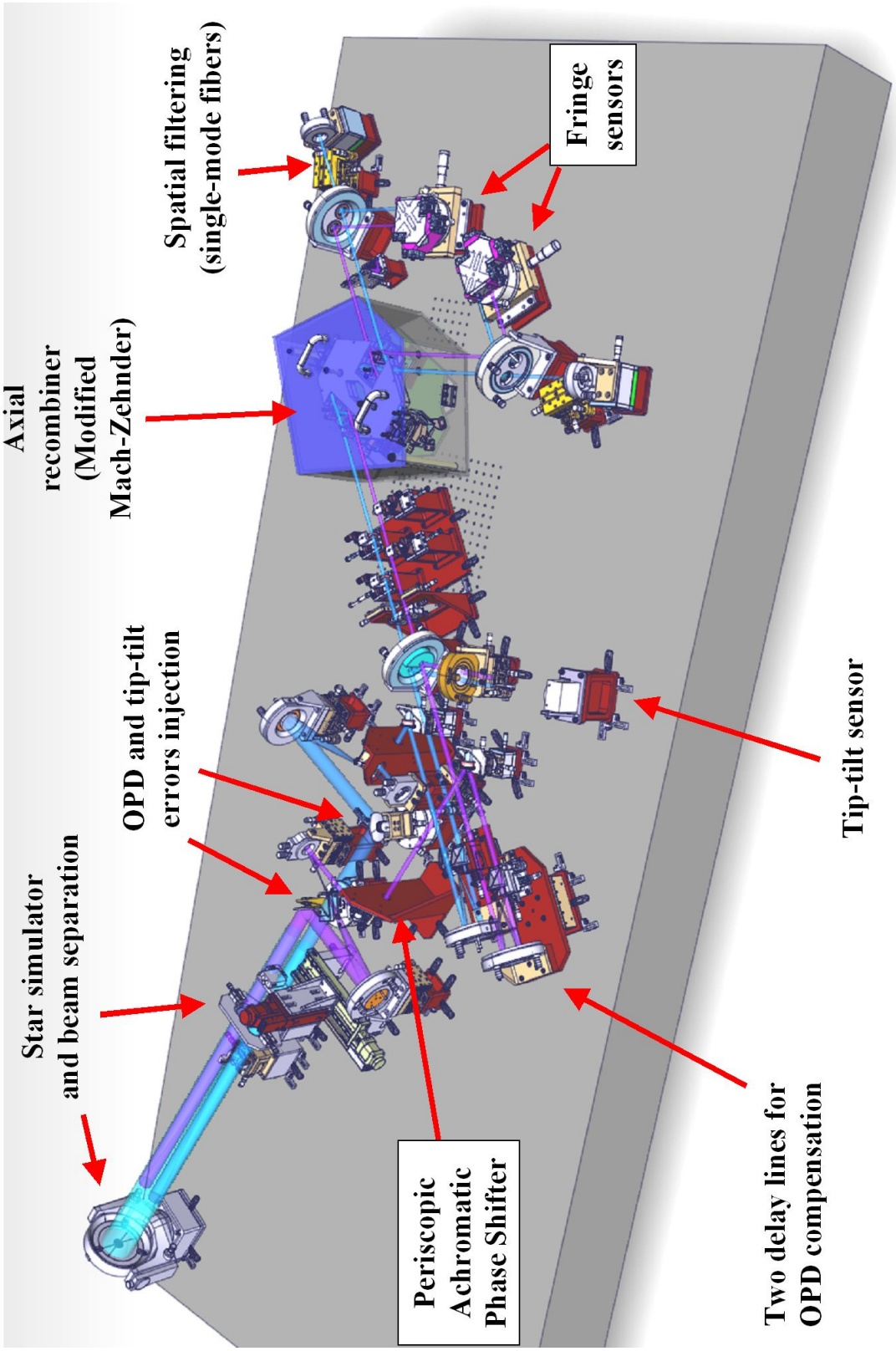

Figure 5: Mechanical implementation of PERSEE interferometer.

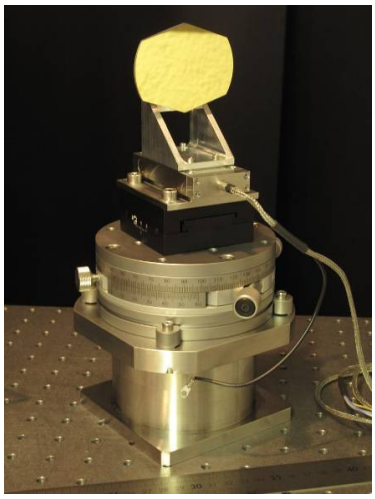

(a)

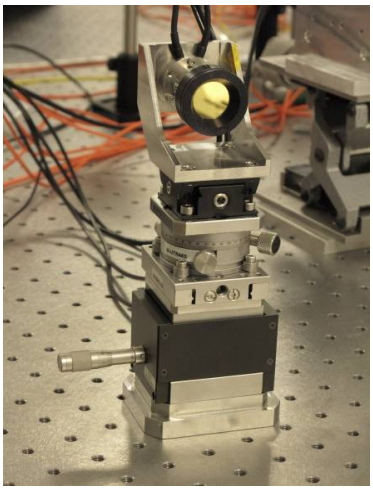

(b)

(c)

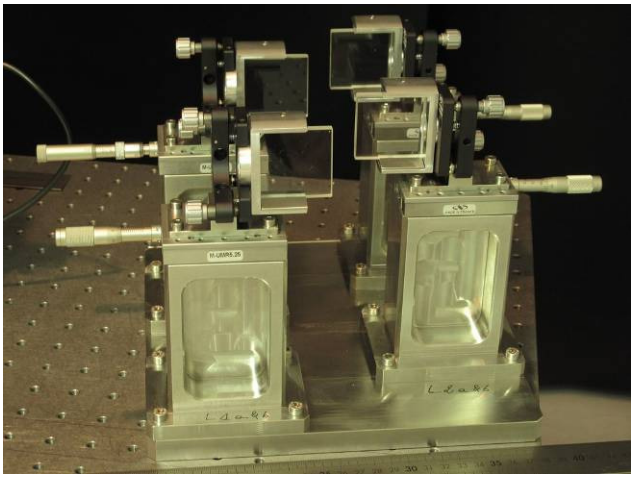

(d)

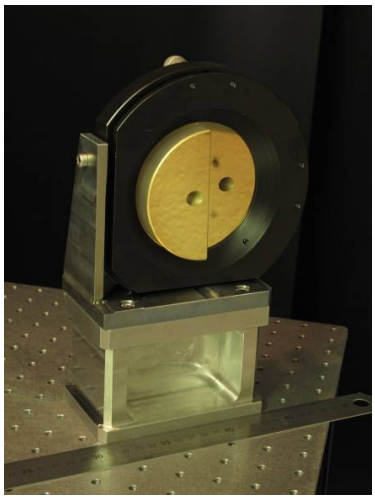

(e)

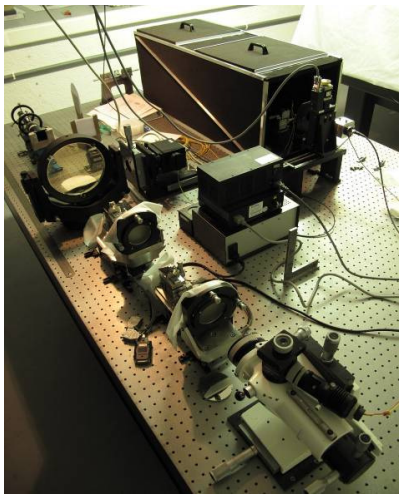

(f)

Figure 6: Pictures from PERSEE main optical train. a) M1 module. b) M6 module. c) Periscope Module. d) Couple of compensating plates. e) M11 mirror. f) Assembled delay line tested on the optical bench.

Depending on the priorities set by the Consortium, the equipment was delivered to the Meudon site in three times, starting first by optical parts located downstream of the MMZ (April 2009), then the light source module (October 2009), and finally the remaining modules representing the most consistent pieces (November 2009). The development of the PERSEE optical bench allowed the team to use and improve their skills and knowledge in a very demanding project and to gain additional experience in the field of nulling interferometry.

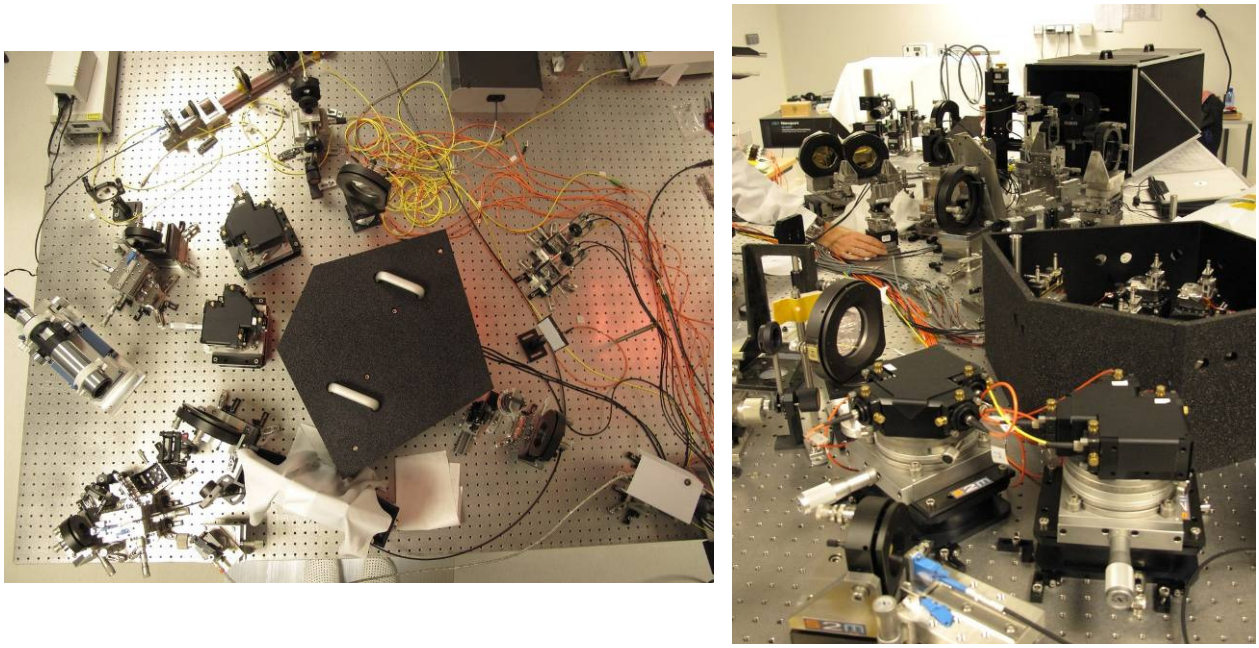

Figure 7: Optical parts and remaining modules downstream the MMZ.

5 CONCLUSION

OCA activities on nulling testbench PERSEE are now being nearly completed, at least from delivery milestones point of view, since all hardware and software have been tested, validated and implemented at the end of year 2009 in the clean rooms of Observatoire de Paris-Meudon. Since then, we continue to participate to the final AIT sequence and to the scientific exploitation of the acquired data, which should run until the end of 2010. Details on the current status of these activities can be found in another paper from this conference [6]. The PERSEE Consortium also plans to open the testbench to other projects involved in nulling interferometry, such as for example NASA's Fourier Kelvin Stellar Interferometer (FKSI): in this perspective, PERSEE could be utilized to quantify the perturbations transmitted by the main truss to the siderostats, thus contributing to validate the mechanical design of the spacecraft.

The authors would like to thank all the other people from the Consortium, and particularly the teams working in IAS (S. Jacquinod, M. Ollivier), ONERA (J. Lozi, F. Cassaing, K. Houairi, B. Sorrente, J. Montri) and LESIA (J.-M. Reess, L. Pham, E. Lhomé, T. Buey, V. Coudé du Foresto) for kind and fructuous cooperation during this four-years project.

REFERENCES

[1] A. Léger, J. M. Mariotti, B. Mennesson, M. Ollivier, J. L. Puget, D. Rouan, J. Schneider, "Could we search for primitive life on extrasolar planets in the near future ? The Darwin project," Icarus 123, p. 249-255 (1996).

[2] "TPF-I Science Working Group Report," JPL Publication 07-1, P. R. Lawson, O. P. Lay, K. J. Johnston and C. A. Beichman eds., Jet Propulsion Laboratory, California Institute of Technology, Pasadena, California (2007).

[3] W. Danchi, R. Barry, P. Lawson, W. Traub, S. Unwin, "The Fourier Kelvin Stellar Interferometer (FKSI): a review, progress report, and update," Proceedings of the SPIE 7013, n° 70132Q (2008).

[4] J.M. Le Duigou, M.Ollivier, A. Léger, F. Cassaing, B. Sorrente, B. Fleury, G. Rousset, O. Absil, D. Mourard, Y. Rabbia, L. Escarrat, F. Malbet, D. Rouan, R. Clédassou, M. Delpech, P. Duchon, B. Meyssignac, P.Y. Guidotti, N. Gorius, "Pegase: a space-based nulling interferometer," Proceedings of the SPIE 6265, n° 62651M (2006).

[5] F. Cassaing, J.M. LeDuigou, J.P. Amans, M. Barillot, T. Buey, F. Hénault, K. Houairi, S. Jacquinod, P. Laporte, A. Marcotto, L. Pirson, J.M. Reess, B. Sorrente, G. Rousset, V. Coudé du Foresto, M. Ollivier, "Persee: a nulling demonstrator with real-time correction of external disturbances," Proceedings of the SPIE 7013, n° 70131Z (2008).

[6] J. Lozi, F. Cassaing, J.M. Le Duigou, K. Houairi, B. Sorrente, J. Montri, S. Jacquinod, J-M Reess, L. Pham, E. Lhomé, T. Buey, F. Hénault, A. Marcotto, P. Girard, N. Mauclert, M. Barillot, V. Coudé du Foresto, M. Ollivier, "PERSEE: Experimental results on the cophased nulling bench," these proceedings.

[7] E. Serabyn, M. M. Colavita, "Fully symmetric nulling beam combiners," Applied Optics 40, p. 1668-1671 (2001).

[8] F. Hénault, "Simple Fourier optics formalism for high angular resolution systems and nulling interferometry," JOSA A 27, p. 435-449 (2010).

[9] S. Jacquinod, F. Cassaing, J.-M. Le Duigou, M. Barillot, M. Ollivier, K. Houairi, F. Lemarquis, J.-P. Amans, "PERSEE: description of a new concept for nulling interferometry recombination and OPD measurement," Proceedings of the SPIE 7013, n° 70131T (2008).

[10] "Dossier justificatif optique de PERSEE," CNES report n° PE-NT-OPT-067-CNES (2008).

[11] F. Hénault, "Computing extinction maps of star nulling interferometers," Optics Express 16, n° 7, p. 4537-4546 (2008).

[12] F. Hénault, "Fine art of computing nulling interferometer maps," Proceedings of the SPIE 7013, n° 70131X (2008).

[13] R. M. Morgan, J. Burge, N. Woolf, "Nulling interferometric beam combiner utilizing dielectric plates: experimental results in the visible broadband," Proceedings of the SPIE 4006, p. 340-348 (2000).

[14] V. Weber, M. Barillot, P. Haguenauer, P. Kern, I. Schanen-Duport, P. Labeye, L. Pujol, Z. Sodnik, "Nulling interferometer based on an integrated optics combiner," Proceedings of the SPIE 5491, p. 842-850 (2004).